Inorg. Chem. **2003**, *42*, 6252–6264

Binding Sites of Nitrogenase: Kinetic and Theoretical Studies of Cyanide Binding to Extracted FeMo-Cofactor Derivatives

Zhen Cui,[†] Adrian J. Dunford,[‡] Marcus C. Durrant,[§] Richard A. Henderson,*[,‡] and Barry E. Smith[†]

Department of Biological Chemistry, John Innes Centre, Colney, Norwich NR4 7UH, U.K., Chemistry, School of Natural Sciences, Bedson Building, University of Newcastle, Newcastle-upon-Tyne NE1 7RU, U.K., and Computational Biology Group, John Innes Centre, Colney, Norwich NR4 7UH, U.K.

Received March 24, 2003

The first kinetic study of a substrate (CN^-) binding to the isolated active site (extracted FeMo-cofactor) of nitrogenase is described. The kinetics of the reactions between CN^- and various derivatives of extracted FeMo-cofactor {FeMoco–L; where L is bound to Mo, and is NMF, Bu^tNC, or imidazole (ImH)} have been followed using a stopped-flow, sequential-mix method in which the course of the reaction is followed indirectly, by monitoring the change in the rate of the reaction of the cofactor with PhS^-. The kinetic results, together with DFT calculations, indicate that the initial site of CN^- binding to FeMoco–L is controlled by a combination of the electron-richness of the cluster core and lability of the Mo–L bond. Ultimately, the reactions between FeMoco–L and CN^- involve displacement of L and binding of CN^- to Mo. These reactions occur with a variety of rates and rate laws dependent on the nature of L. For FeMoco–NMF, the reaction with CN^- is complete within the dead-time of the apparatus (ca. 4 ms), while with FeMoco–$CNBu^t$ the reaction is much slower and exhibits first order dependences on the concentrations of both FeMoco–$CNBu^t$ and CN^- ($k = 2.5 \pm 0.5 \times 10^4$ dm^3 mol^{-1} s^{-1}). The reaction of FeMoco–ImH with CN^- occurs at a rate which exhibits a first order dependence on FeMoco–ImH but is independent of the concentration of CN^- ($k = 50 \pm 10$ s^{-1}). The results are interpreted in terms of CN^- binding directly to the Mo site for FeMoco–NMF and FeMoco–ImH, but with FeMoco–$CNBu^t$ initial binding at an Fe site is followed by movement of CN^- to Mo. Complementary DFT calculations are consistent with this interpretation, indicating that, in FeMoco–L, the Mo–L bond is stronger for L = ImH than for L = $CNBu^t$ and the binding of CN^- to Mo is stronger than to any Fe atom in the cofactor.

Introduction

The nitrogenases are a family of metalloenzymes which convert dinitrogen into ammonia by sequences of coupled electron- and proton-transfer reactions.[1,2] Three types of nitrogenases have been identified and are distinguished by their metal content.[3] The most thoroughly studied type is that based on Mo, and in the other enzymes, Mo is replaced by V or Fe. All nitrogenases comprise two metalloproteins. The smaller of the two proteins is the Fe-protein (mol wt = ca. 60 000) which contains a single cuboidal $\{Fe_4S_4\}$ cluster and mediates electron transfer from the external reductant (a flavodoxin or ferredoxin) to the larger protein. In the Mo-based nitrogenase, this larger protein is called the MoFe-protein (mol wt = ca. 230 000). The MoFe-protein has an $\alpha_2\beta_2$ structure[4] and contains two structurally unique Fe−S-based clusters: (i) the so-called P-clusters which have a $\{Fe_8S_7\}$ core, and may be electron storage sites, and (ii) the substrate-binding and reducing sites which have a composition $MoFe_7S_9$(*R*-homocitrate) and are referred to as FeMo-cofactor (Figure 1). The cofactor is bound to the polypep-

* To whom correspondence should be addressed. E-mail: r.a.henderson@ncl.ac.uk.
[†] Department of Biological Chemistry, John Innes Centre.
[‡] University of Newcastle.
[§] Computational Biology Group, John Innes Centre.

(1) Smith, B. E. In *Advances in Inorganic Chemistry*; Sykes, A. G., Cammack, R., Eds.; Academic Press: London, 1999; Vol 47, pp 160−218 and references therein.
(2) Evans, D. J.; Henderson, R. A.; Smith, B. E. *Bioinorganic Catalysis*, 2nd ed.; Reedijk, J., Bouwman, E., Eds.; Marcel Dekker: New York, 1999; Chapter 7 and references therein.
(3) Eady, R. R. *Chem. Rev.* **1996**, *96*, 3013 and references therein.
(4) Lawson, D. M.; Smith, B. E. In *Metal Ions in Biological Systems*; Sigel, A., Sigel, H., Eds.; Marcel Dekker: New York, 2002; Vol. 39, Chapter 3 and references therein.

10.1021/ic030108q CCC: $25.00
Published on Web 09/03/2003

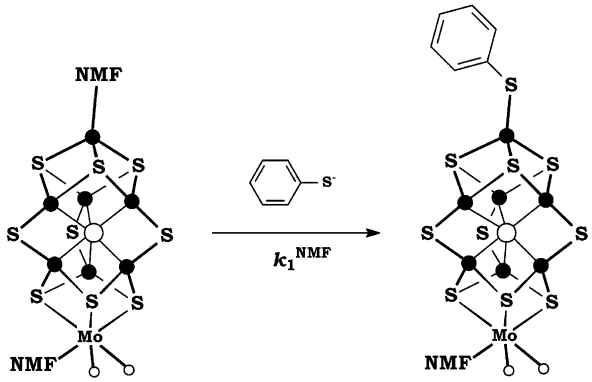

Figure 1. Reporter reaction used throughout this study to monitor the status of extracted FeMo-cofactor: the reaction of an excess of PhS^- with extracted FeMo-cofactor. (Here, and in the other figures, Fe = ●, and the recently discovered central light atom[5] is represented by ○.)

tide[2,4] at the unique tetrahedral Fe by a thiolate sulfur of Cysα273, and to the octahedral Mo by the imidazole residue of Hisα440 (the amino acid numbering refers to the *Klebsiella pneumoniae* MoFe-protein crystal structure). The remaining 6 Fe atoms in the cofactor are all contained in the central portion of the cluster. Recently, a very high resolution (1.16 Å) structure of the MoFe protein has been reported.[5] The data indicate that a single light atom (N, C, or O) sits in the center of the FeMo-cofactor and is bonded to each of the 6 central Fe atoms. The significance of this intriguing finding has not yet been established.

In addition to dinitrogen, nitrogenases also transform C_2H_2, N_2O, N_3^-, cyclopropene, MeNC, CN^-, and H^+. While it is generally accepted that FeMo-cofactor is the site where all these substrates are bound and converted into product,[1−4] there is a growing body of circumstantial evidence that different substrates bind at different redox states and possibly different areas of the FeMo-cofactor. How and where any of these substrates bind to this cluster remains contentious. There are three general areas on cofactor where substrates could in principle bind: the tetrahedral Fe, the girdle of 6 Fe atoms in the center of the cluster, and the Mo atom. Several groups[6] have used quantum calculations of widely varying degrees of sophistication to examine the possible coordination modes for dinitrogen bound to FeMo-cofactor. While all agree that the tetrahedral Fe can be excluded as a possible binding site, no unified picture as to the actual binding site and subsequent pathway for dinitrogen reduction has yet emerged. Most of the studies focus on dinitrogen binding to one or more of the Fe atoms in the center of the cofactor. However, some recent calculations[6b] have indicated that the Mo atom is a more favored binding site than Fe provided the Mo can attain a coordination number lower than six. Clearly, there is a need for experimental approaches to probe where substrates bind on FeMo-cofactor.

FeMo-cofactor can be extracted intact[7] from the MoFe-protein and into the organic solvent, *N*-methylformamide (NMF). Studies on extracted FeMo-cofactor complement those on the enzyme by focusing on the intimate reactions of this structurally unique cluster. The Fe−cysteinate and Mo−histidine bonds must be cleaved during the extraction, and it is reasonably assumed that solvent occupies these two positions in the extracted FeMo-cofactor. It seems likely that these coordinated solvent molecules are labile, and thus, species such as L = CN^-, N_3^-, and RNC, which are known[8] to bind to extracted FeMo-cofactor (to form FeMoco−L) can do so at any of the metal atoms on the cluster. In principle, the results from kinetic studies on the reactions between extracted FeMo-cofactor and L can indicate how and where substrates bind to the cluster. In practice, no such studies have been reported because the reactions are rapid, and binding of substrates to extracted FeMo-cofactor is often associated with small spectroscopic changes making the reactions difficult to follow. Herein, we describe a general method for monitoring these fundamental reactions and report the first study of the kinetics of a nitrogenase substrate (CN^-) binding to extracted FeMo-cofactor (FeMoco−NMF) and two cofactor derivatives containing bound Bu^tNC (FeMoco−$CNBu^t$) or imidazole (FeMoco−ImH). We have also performed DFT calculations on sytsems which model fragments of the cofactor. These calculations complement our kinetic studies, and together, the results indicate that CN^- binds to the Mo of FeMoco−L by displacing L, but that the mechanism by which CN^- ends up on Mo depends on the nature of L in the FeMo-cofactor derivative.

Experimental Section

All manipulations involving the preparation and handling of solutions of extracted FeMo-cofactor were performed under an atmosphere of dinitrogen in a glovebox operating at less than 1 ppm dioxygen. The compounds Bu^tNC, imidazole, and $[NEt_4]CN$ were purchased from Aldrich and used as received.

Preparation of Materials. The nitrogenase MoFe-protein was purified from wild-type *Klebsiella pneumoniae* M5a1, and the FeMo-cofactor was isolated and assayed using minor modifications of the procedures described in the literature.[7,9] $[NEt_4]SPh$ was prepared by the literature method[10] and recrystallized from MeCN/Et_2O. Its purity was checked by ^1H NMR spectroscopy. NMF was purchased from Aldrich, dried over anhydrous sodium carbonate, and distilled under reduced pressure using a rotary evaporator.

(5) Einsle, O.; Teczan, F. A.; Andrade, S. L. A.; Schmid, B.; Yoshida, M.; Rees, D. C. *Science* **2002**, *297*, 1696.
(6) For recent theoretical papers and commentary on earlier work see: (a) Rod, T. H.; Nørskov, J. K. *J. Am. Chem. Soc*. **2000**, *122*, 12751. (b) Durrant, M. C. *Biochemistry* **2002**, *41*, 13934. (c) Lovell, T.; Li, J.; Case, D. A.; Noodleman, L. *J. Am. Chem. Soc.* **2002**, *124*, 4546.
(7) (a) Shah, V. K.; Brill, W. J. *Proc. Natl. Acad. Sci. U.S.A.* **1997**, *74*, 3249. (b) Burgess, B. K. *Chem. Rev.* **1990**, *90*, 377 and refs therein.
(8) A variety of different studies indicate the binding of certain small molecules and ions to extracted FeMo-cofactor. Leading references include the following: (a) Liu, H. I.; Filipponi, A.; Gavini, N.; Burgess, B. K.; Hedman, B.; di Cicco, A.; Natoli, C. R.; Hodgson, K. O. *J. Am. Chem. Soc*. **1994**, *116*, 2418. (b) Conradson, S. D.; Burgess, B. K.; Vaughn, S. A.; Roe, A. L.; Hedman, B.; Hodgson, K. O.; Holm, R. H. *J. Biol. Chem.* **1989**, *264*, 15967. (c) Schultz, F. A.; Feldman, B. J.; Gheller, S. F.; Newton, W. E. *Inorg. Chim. Acta* **1990**, *170*, 115. (d) Newton, W. E.; Gheller, S. F.; Feldman, B. J.; Dunham, W. R.; Schultz, F. A. *J. Biol. Chem.* **1989**, *264*, 1924. (e) Richards, A. J. M.; Lowe, D. J.; Richards, R. L.; Thomson, A. J.; Smith, B. E. *Biochem. J.* **1994**, *297*, 373 and refs therein.
(9) McLean, P. A.; Wink, D. A.; Chapman, S. K.; Hickman, A. B.; McKillop, D. M.; Orme-Johnson, W. H. *Biochemistry* **1989**, *28*, 9402 and references therein.
(10) Palermo, R. E.; Power, P. P.; Holm, R. H. *Inorg. Chem.* **1982**, *21*, 173.

Kinetic Studies. Solutions of extracted FeMo-cofactor (1×10^{-4} mol dm^{-3}) were prepared in a glovebox using NMF containing sodium dithionite (1×10^{-3} mol dm^{-3} added in aqueous solution containing 5×10^{-3} mol dm^{-3} phosphate buffer, pH 8) as the solvent.[7,9] The solution was loaded into a 5 mL all-glass syringe inside the glovebox and stoppered with a needle attached to a rubber bung. The sealed syringe was then removed from the glovebox and loaded into the stopped-flow, sequential-mix apparatus, without allowing air to come into contact with the cofactor solution.

The FeMo-cofactor derivatives, FeMoco−$CNBu^t$ and FeMoco−ImH, were prepared in the glovebox by adding 5−10 mol equiv of Bu^tNC or imidazole, respectively, to an NMF solution of FeMo-cofactor as extracted.

The kinetics of the reactions between extracted FeMo-cofactor (and its derivatives) were measured on an Applied Photophysics SX.18MV stopped-flow spectrophotometer modified to handle air-sensitive solutions. The temperature was maintained at 25.0 °C using a Grant LTD6G thermostat tank. The kinetics were studied at $\lambda =$ 460 nm, and the values of the observed rate constants (k_{obs}) were determined by curve-fitting of the absorbance−time trace using the Applied Photophysics software on the computer interfaced to the stopped-flow spectrophotometer. Analyses of the dependence of the observed rate constants on the concentration of CN^- are described in the Results and Discussion section.

DFT Studies. All DFT calculations were carried out using the B3LYP hybrid functional and LanL2DZ basis set as implemented in GAUSSIAN 98W.[11] Geometry optimizations were carried out using partial *z*-matrix methods. For the tetrahedral Fe site, the S−Fe−S angles were constrained to 105.4°, the mean value from the *K. pneumoniae* X-ray crystal structure,[12] and the rest of the structure was allowed to refine freely. For the $[(HS)Fe(SH)_2Mo(SH)(OCH_2CO_2)]$ model, the metal−sulfur section was treated as having a plane of symmetry lying through the Fe and Mo atoms and the terminal SH groups, and the glycolate ligand was allowed to refine freely. The effects of introducing other geometrical restraints are described in the following text. For this model, the default geometry optimization convergence criteria proved unsatisfactory with very slow convergence associated with insignificant energy changes. Geometry optimizations were therefore terminated when the change in energy over 10 successive minima was less than 0.1 kcal mol^{-1}.

Results and Discussion

Extracted FeMo-cofactor binds a variety of molecules and ions, including some of the substrates of nitrogenase (L = H^+, CN^-, N_3^-, and RNC);[8] however, following the time course of these reactions is not simple. The binding of molecules and ions to extracted FeMo-cofactor is fast and must be studied using the stopped-flow technique where reactions with half-lives longer than 2 ms can be followed. The vast majority of stopped-flow apparatuses monitor reactions using spectrophotometry, and this is a problem in the study of substrate binding to extracted FeMo-cofactor. The UV−vis absorption spectra of FeMo−L are indistinguishable from that of FeMo-cofactor as extracted (FeMoco−NMF). The "spectrophotometrically silent" nature of the reactions between FeMoco−NMF and L has for a long time precluded their study. We have now developed a kinetic method which detects when L is bound to cofactor.[13] In the remainder of this paper, we show how this approach has been used to measure the kinetics of CN^- binding to the FeMoco−NMF and its derivatives, FeMoco−ImH (ImH = imidazole) and FeMoco−$CNBu^t$.

Extracted FeMo-Cofactor. It is important to clarify some features about extracted FeMo-cofactor prior to discussion of its reactivity. In the absence of a crystal structure, we assume that extracted FeMo-cofactor is as shown in Figure 1 with an interstitial[5] N, C, or O atom. EXAFS studies have shown[14] that the dimensions of cofactor in the extracts are essentially unchanged from those of cofactor in the protein. It seems likely, since the Mo of cofactor is 6-coordinate in the protein, that this coordination number is retained in the extracts. Our earlier studies[13b] showed that the cofactors extracted from wild type and $NifV^-$ nitrogenases have different reactivities in the presence of imidazole, consistent with *R*-homocitrate being bound to Mo even in the extracts. The main contentious issue is what else is bound to Mo. A variety of species are used in the extraction procedure (e.g. Cl^-, HPO_4^{2-}, $S_2O_4^{2-}$, etc.), and any of these could be bound. For simplicity, throughout this paper we will assume that FeMo-cofactor as extracted contains NMF (i.e., solvent molecules) bound to both the tetrahedral Fe and Mo. Our experimental proceedure for isolating FeMo-cofactor is always the same. Consequently, if we are mistaken and another molecule is bound to Mo, the interpretations of our kinetic results will not be affected, only the identity of the Mo ligation.

It has been proposed that extracted FeMo-cofactor exists as oligomers.[15] However, we have seen no evidence of this in our kinetic studies.[13] Thus, in our previous kinetic studies, dilution of the cofactor solutions did not lead to changes in the rate of reaction. If oligomers are present, then either their reactivities with PhS^- are indistinguishable, or the rate of interconversion between unreactive and reactive forms is more rapid than the reactions studied herein.

The Kinetic Method. When FeMo-cofactor as extracted (FeMoco−NMF) reacts with an excess of PhS^- in NMF

(11) Frisch, M. J.; Trucks, G. W.; Schlegel, H. B.; Scuseria, G. E.; Robb, M. A.; Cheeseman, J. R.; Zakrzewski, V. G.; Montgomery, J. A., Jr.; Stratmann, R. E.; Burant, J. C.; Dapprich, S.; Millam, J. M.; Daniels, A. D.; Kudin, K. N.; Strain, M. C.; Farkas, O.; Tomasi, J.; Barone, V.; Cossi, M.; Cammi, R.; Mennucci, B.; Pomelli, C.; Adamo, C.; Clifford, S.; Ochterski, J.; Petersson, G. A.; Ayala, P. Y.; Cui, Q.; Morokuma, K.; Malick, D. K.; Rabuck, A. D.; Raghavachari, K.; Foresman, J. B.; Cioslowski, J.; Ortiz, J. V.; Stefanov, B. B.; Liu, G.; Liashenko, A.; Piskorz, P.; Komaromi, I.; Gomperts, R.; Martin, R. L.; Fox, D. J.; Keith, T.; Al-Laham, M. A.; Peng, C. Y.; Nanayakkara, A.; Gonzalez, C.; Challacombe, M.; Gill, P. M. W.; Johnson, B. G.; Chen, W.; Wong, M. W.; Andres, J. L.; Head-Gordon, M.; Replogle, E. S.; Pople, J. A. *Gaussian 98*, revision A.7; Gaussian, Inc.: Pittsburgh, PA, 1998.
(12) Mayer, S. M.; Lawson, D. M.; Gormal, C. A.; Roe, S. M.; Smith, B. E. *J. Mol. Biol.* **1999**, *292*, 871.
(13) (a) Grönberg, K. L. C.; Gormal, C. A.; Smith, B. E.; Henderson, R. A. *J. Chem. Soc., Chem. Commun.* **1997**, 713. (b) Grönberg, K. L. C.; Gormal, C. A.; Durrant, M. C.; Smith, B. E.; Henderson, R. A. *J. Am. Chem. Soc.* **1998**, *120*, 10613.
(14) (a) Conradson, S. D.; Burgess, B. K.; Newton, W. E.; Mortensen, L. E.; Hodgson, K. O. *J. Am. Chem. Soc.* **1987**, *109*, 7507. (b) Arber, J. M.; Flood, A. C.; Garner, C. D.; Gormal, C. A.; Hasnain, S. S.; Smith, B. E. *Biochem. J.* **1988**, *252*, 421.
(15) (a) Huang, H. Q.; Kofford, M.; Simpson, F. B.; Watt, G. D. *J. Inorg. Biochem.* **1993**, *52*, 59. (b) Frank, P.; Angove, H. C.; Burgess, B. K.; Hodgson, K. O. *JBIC, J. Biol. Inorg. Chem.* **2001**, *6*, 683.

solution, only one thiolate binds to the cluster.[7b,16] EXAFS studies show that the thiolate is bound to an Fe center. It seems most likely that this is the unique tetrahedral Fe,[17] as shown in Figure 1, since, of all the Fe atoms in FeMo-cofactor, only the tetrahedral Fe has a natural affinity for binding thiolates (i.e., Cysα273 in the MoFe-protein).

The reaction between FeMoco−NMF and PhS^- is associated with a change in the visible absorption spectrum around $\lambda = 450-480$ nm and is readily monitored by stopped-flow spectrophotometry.[13] The kinetics of the reaction exhibit a first order dependence on the concentration of cofactor but are independent of the concentration of PhS^-, consistent with a dissociative substitution mechanism. The rate of the reaction with PhS^- (k_1^{NMF}) is sensitive to what is bound to the cofactor. Thus, for derivatives of extracted FeMo-cofactor (FeMoco−L), the rate of the reaction with PhS^- (k_1^L) is different from k_1^{NMF}. It is the sensitivity of k_1^L to what is bound to the cofactor which is the basis of our approach to monitoring the time course of L binding to the cofactor. Our earlier kinetic studies on extracted FeMo-cofactor[13] indicated that changes to the ligation at Mo result in changes to the rate of substitution at the tetrahedral Fe site, some six bonds away. Although the change in rate is modest (e.g., the difference in the rate of reaction of PhS^- with FeMoco−NMF and FeMoco−ImH is only about a factor of 2), it is easily discernible.

To measure the kinetics of a substrate (L) binding to extracted FeMo-cofactor, we have developed a stopped-flow, sequential-mix approach as represented in Figure 2. In a typical experiment, solutions of FeMoco−L and CN^- are rapidly mixed and held together for a known length of time (δ). Subsequently, this solution is mixed with a solution of $[NEt_4]SPh$ whereupon the thiolate reacts with the cofactor. The rate of the reaction between FeMo-cofactor and PhS^- effectively reports on the status of the cofactor. Thus, if δ is small, CN^- will not have reacted with the cofactor, and the rate will correspond to that of FeMoco−L (k_1^L). However, when δ is large, there will have been sufficient time for CN^- and the cofactor to react, and the rate of the reaction with PhS^- will correspond to that of FeMoco−CN (k_1^{CN}). By monitoring how the rate of the reaction with PhS^- varies with δ, the time course for the spectrophotometrically silent reaction between the cofactor and CN^- can be mapped out.

In principle, our approach can be used to monitor the binding of *any* substrate (L) to extracted FeMo-cofactor; in practice, its application is limited. During the stopped-flow, sequential-mix experiments, the cofactor solution is diluted 4-fold before it is analyzed: initial equivolume mixing with the solution of CN^- is followed by equivolume mixing with the PhS^- solution. Consequently, the solution of the cofactor being analyzed is only half the concentration of a conventional stopped-flow experiment, and thus, the absorbance−time curves are only half the magnitude. In addition, when

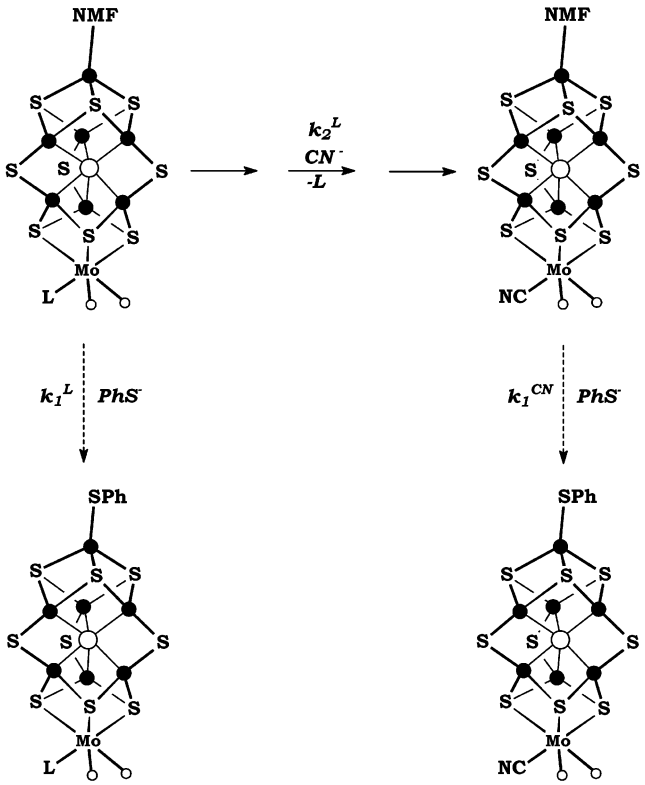

Figure 2. Basic reactions of the stopped-flow, sequential-mix experiments to determine the kinetics of the reactions between FeMoco−L (L = NMF, CNBut, or imidazole) and CN^-.

configured in the sequential-mix mode, the dead time of the apparatus is about 3−4 ms, which is more than double that of the stopped-flow configuration and leads to loss of some of the absorbance change for more rapid reactions. The consequence of both these limitations is that (compared to conventional stopped-flow spectrophotometry) the data from stopped-flow, sequential-mix experiments are associated with a poorer signal-to-noise ratio. It is therefore essential that, in the reaction of FeMoco−NMF with L, the reactant (FeMoco−NMF) and the product (FeMoco−L) react with PhS^- at markedly different rates. The rate of the reaction of PhS^- with FeMoco−CN[11a] is slower {$k_1^{CN} = 2.4 \pm 0.2\ s^{-1}$; eq 1} than that with any other derivative, FeMoco−L (L = N_3, Bu^tNC, imidazole, or NMF). Figure 3 illustrates how easy it is to identify when CN^- is bound to cofactor in the reaction between FeMoco−$CNBu^t$ and CN^- using the stopped-flow, sequential-mix approach.

$$\frac{-\mathrm{d[FeMoco-CN]}}{\mathrm{d}t} = \{(1.35 \pm 0.1) + (4.3 \pm 0.4 \times 10^2)[PhS^-]\}[\mathrm{FeMoco-CN}] \quad (1)$$

Figure 3 shows absorbance−time curves obtained in stopped-flow, sequential-mix experiments after PhS^- (2.5 mmol dm^{-3}) has been added to a mixture of FeMoco−$CNBu^t$ (0.05 mmol dm^{-3}) and CN^- ([CN^-] = 0.5 mmol dm^{-3}). After mixing FeMoco−$CNBu^t$ and CN^-, then leaving for 10 ms, there has been insufficient time for the cofactor to react with the CN^-, and the addition of PhS^- at this time results in a rate which corresponds to that of FeMoco−$CNBu^t$

(16) Rawlings, J.; Shah, V. K.; Chisnell, J. R.; Brill, W. J.; Zimmerman, R.; Münck, E.; Orme-Johnson, W. H. *J. Biol. Chem.* **1978**, *253*, 1001.
(17) Harvey, I.; Strange, R. W.; Schneider, R.; Gormal, C. A.; Garner, C. D.; Hasnain, S. S.; Richards, R. L.; Smith, B. E. *Inorg. Chim. Acta* **1998**, *150*, 275.

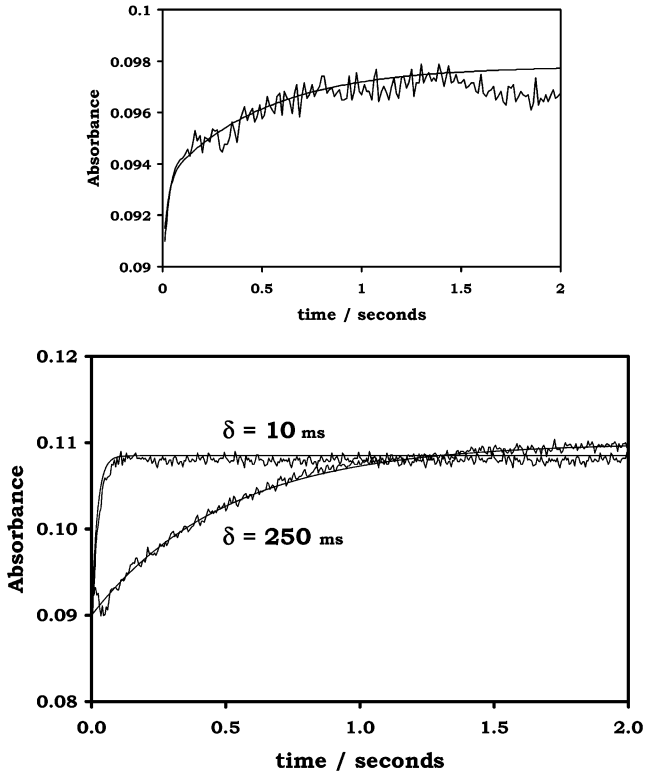

Figure 3. Bottom: Absorbance−time curves showing the reaction of PhS^- (2.5 mmol dm^{-3}) with FeMoco−$CNBu^t$ and CN^- ([CN^-] = 0.5 mmol dm^{-3}). Traces were recorded at δ = 10 ms and δ = 250 ms. The smooth curve fits are single exponentials with corresponding rate constants k_{obs} = 50 s^{-1} and k_{obs} = 2 s^{-1}. Top: Absorbance−time curves for the reaction of PhS^- (2.5 mmol dm^{-3}) with FeMoco−$CNBu^t$ and CN^- ([CN^-] = 0.5 mmol dm^{-3}). Trace recorded at δ = 46 ms. The smooth curve fit is to two exponentials of equal magnitude and rate constants k = 50 s^{-1} and k = 2 s^{-1}.

($k_{obs} = k_1^{CNBu} = 60 \pm 10$ s^{-1}). However, after mixing FeMoco−$CNBu^t$ and CN^-, then leaving for 250 ms, FeMoco−CN has been formed, and so addition of PhS^- at this time results in a rate which corresponds to that of FeMoco−CN ($k_{obs} = k_1^{CN} = 2$ s^{-1}). The values of k_1^{CNBu} and k_1^{CN} obtained in this work are in good agreement with the values established earlier.[13]

Figure 3 (bottom) shows the absorbance−time curves observed at times when either FeMoco−$CNBu^t$ or FeMoco−CN are essentially the only cofactor species present. At intermediate times, when 250 > δ > 10 ms, mixtures of FeMoco−$CNBu^t$ and FeMoco−CN are present. Under these conditions, the absorbance−time traces are biphasic, as shown in Figure 3 (top). The trace is a good fit to two exponentials with rate constants k_{obs} = 50 and 2 s^{-1}, and (as expected) the magnitude of the two phases apparently depends on the value of δ. Thus, when δ corresponds to approximately the half-life of the reaction ($t_{1/2}$ = 56 ms, δ = 46 ms, [CN^-] = 0.5 mmol dm^{-3}), each phase contributes equally to the total absorbance change. The biphasic behavior is difficult to detect when δ corresponds to about 10−20% or 80−90% completion. Under these conditions, the absorbance−time curves can be fitted to single exponentials, with rate constants corresponding to the dominant species, FeMoco−$CNBu^t$ or FeMoco−CN, respectively. The quality of the data is not sufficiently good to allow deconvolution of the absorbance changes, at different values of δ, into their component exponentials.

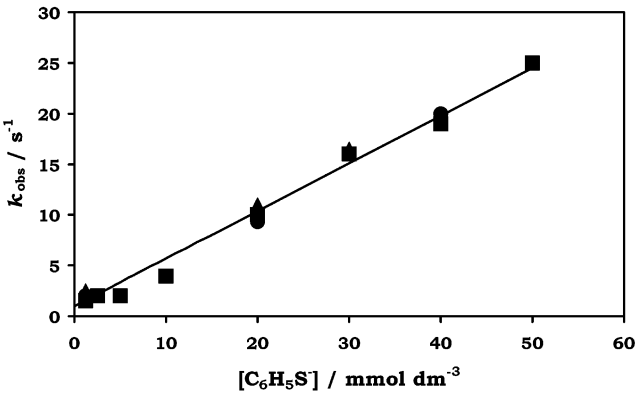

Figure 4. Kinetic data for the reaction of PhS^- with the products of the reactions between CN^- and FeMoco−L (L = NMF, Bu^tNC or imidazole), measured in NMF at 25.0 °C. Data points correspond to studies with FeMoco−NMF (■); FeMoco−$CNBu^t$ (●); and FeMoco−Im (▲). The line is that defined by eq 1.

The Products of the Reactions between CN^- and FeMoco−L (L = Bu^tNC, NMF, or Imidazole). We have used the rates of the reactions with PhS^- to identify the products formed in the reactions between the various FeMoco−L (L = NMF, Bu^tNC or imidazole) and CN^-. Figure 4 shows that the products of the reactions between *all* FeMoco−L and an excess of CN^- react with PhS^- at the same rate. The line drawn in Figure 4 is defined by eq 1 and is that established in earlier work on the reaction of PhS^- with FeMoco−CN (produced from the reaction of CN^- with the cofactor extracted from either the wild-type or $NifV^-$ enzyme[13b]). On the basis of these results, it seems likely that all of the FeMoco−L derivatives react with CN^- to give the same product, FeMoco−CN, via dissociation of L, as shown in eq 2.

$$\text{FeMoco}-\text{L} + CN^- \rightarrow \text{FeMoco}-\text{CN} + \text{L} \qquad (2)$$

Central to our interpretation of the kinetics is the assignment that imidazole is bound to Mo. Earlier work[13a] indicated that Bu^tNC in FeMoco−$CNBu^t$ and imidazole in FeMoco−ImH are bound to Mo. In both cases, the proposal that Mo is the binding site is circumstantial (since we have no structural confirmation) but is a reasonable assignment. Thus, the Mo in FeMo-cofactor has a natural affinity for binding imidazole (Hisα440) in the MoFe-protein.[1,4] In addition, wild-type FeMoco−ImH (containing *R*-homocitrate coordinated to Mo) and $NifV^-$ FeMoco−ImH (containing citrate coordinated to Mo) have different reactivities.[13b] This unique difference in reactivity is only rationalizable if the imidazole is coordinated to Mo and interacts differently with the two polycarboxylates. The evidence that Bu^tNC is bound to Mo is based on the interpretation of earlier kinetic results.[13a]

Kinetics of the Reaction between CN^- and FeMoco−L (L = NMF, Bu^tNC, or Imidazole). Before discussing the kinetics of the reactions between FeMoco−L and CN^-, we need to distinguish between kinetically and thermodynamically favored binding sites. The results presented in Figure 4 indicate that CN^- binds ultimately to Mo (i.e., Mo is the

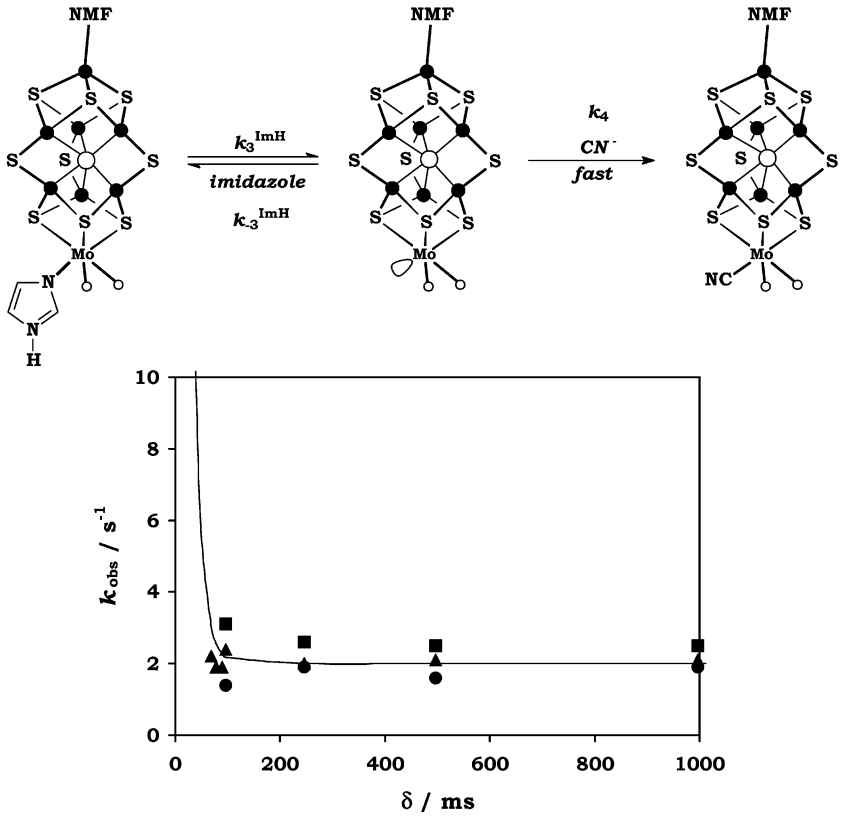

Figure 5. Kinetic data for the reaction of FeMoco−ImH (0.025 mmol dm^{-3}) and an excess of CN^- determined using the stopped-flow, sequential-mix approach in which the time course of the reaction (δ) is monitored by changes in the rate of reaction (k_{obs}) of the cofactor with PhS^- (2.5 mmol dm^{-3}). The data points correspond to studies where [CN^-] = 0.25 (■), 0.5 (●), or 1.0 mmol dm^{-3} (▲). The curve drawn is defined by $(k_{obs})_\delta = 2 + 90\exp(-50\delta)$.

thermodynamically favored binding site). However, only kinetic studies will show if CN^- binds directly to this site, or if CN^- binds preferentially to another site (kinetically favored binding site) and subsequently moves to Mo. First, we will discuss the kinetics of the reaction between FeMoco−ImH and CN^-, where CN^- appears to bind directly to Mo, and then we will consider the analogous reactions of FeMoco−NMF and FeMoco−$CNBu^t$. We will present evidence indicating that CN^- binds initially to FeMoco−$CNBu^t$ at an Fe site, and subsequently moves to Mo.

(a) FeMoco−ImH. The kinetic data for the reaction between CN^- and FeMoco−ImH are shown in Figure 5. The δ axis corresponds to the time that FeMoco−ImH and CN^- have been left together after mixing. The k_{obs} axis shows the rate constants for the reaction of PhS^- with the mixtures of FeMoco−ImH and CN^- after the time δ. Thus, the k_{obs} axis is effectively a measure of the status of the cluster (i.e., what is bound to FeMo-cofactor). If PhS^- is added when δ < 10 ms, the reaction is very fast, and only the tail end of the absorbance−time curve is observed (Figure 6). Earlier studies[13a] have shown that the reaction of PhS^- with FeMoco−ImH is rapid ($k_{obs} = k_1^{ImH} = 95 \pm 10\ s^{-1}$). This reaction is on the limit of the stopped-flow, sequential-mix technique, and so we assume that the rapid reaction shown in Figure 6 corresponds to that of PhS^- with FeMoco−ImH. If PhS^- is added when δ = ca. 100 ms, a single-exponential absorbance−time curve is observed with k_{obs} corresponding to that of FeMoco−CN ($k_{obs} = k_1^{CN} = 2\ s^{-1}$). Experiments in which the concentration of CN^- has varied ([CN^-] = 0.25−1.0 mmol dm^{-3}) showed that FeMoco−CN is always produced at δ = ca. 100 ms, indicating the rate of the reaction between FeMoco−ImH and CN^- is independent of the concentration of CN^- ($k_{obs} = 50 \pm 10\ s^{-1}$). The rate of the reaction between FeMoco−ImH and CN^- is unaffected by the concentration of free imidazole present in solution ([ImH] = 0.4−2.0 mmol dm^{-3}).

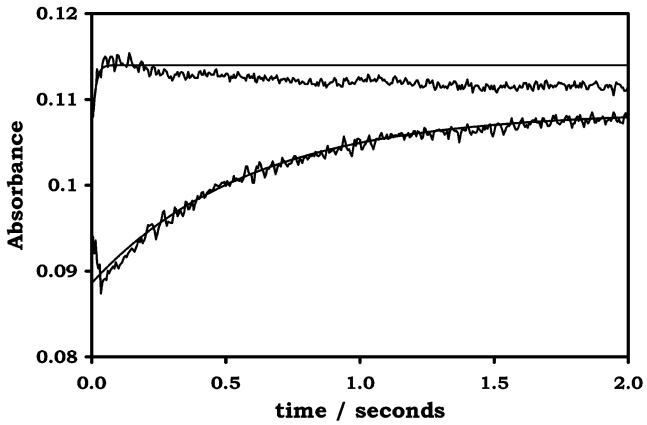

Figure 6. Absorbance−time curves showing the reaction of PhS^- (2.5 mmol dm^{-3}) with FeMoco−ImH and CN^- ([CN^-] = 0.5 mmol dm^{-3}). Traces were recorded at δ = 13 ms (top) and δ = 200 ms (bottom). The smooth curve fits are single exponentials with corresponding rate constants $k_{obs} = 90\ s^{-1}$ and $k_{obs} = 2\ s^{-1}$.

The kinetics observed for the reaction between FeMoco−ImH and CN^- are unique to this cofactor derivative and are consistent with a unimolecular reaction. The unimolecular

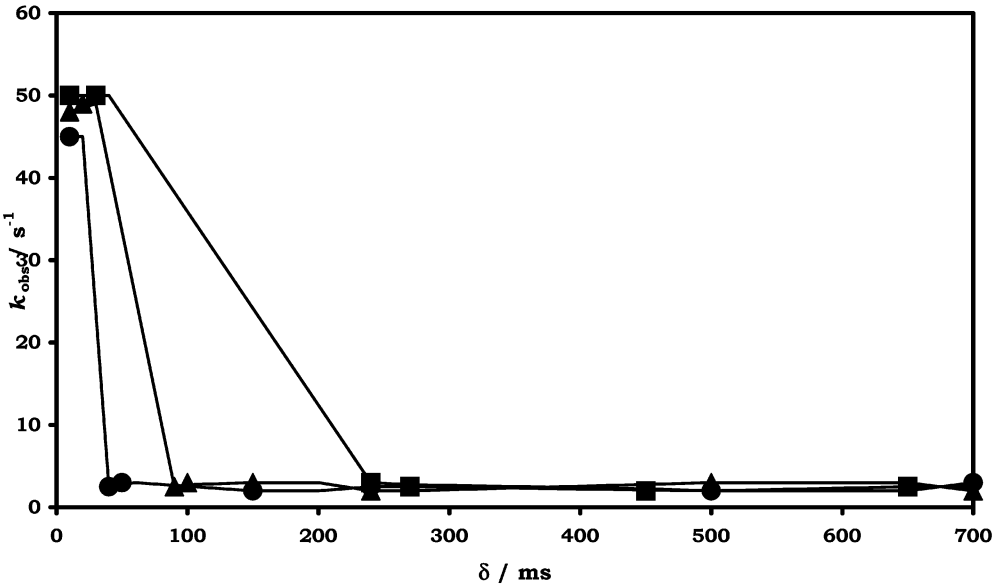

Figure 7. Kinetic data for the reaction of FeMoco−CNBu^t (0.025 mmol dm^{-3}) and an excess of CN^- determined using the stopped-flow, sequential-mix approach in which the time course of the reaction (δ) is monitored by changes in the rate of reaction (k_{obs}) of the cofactor with PhS^- (2.5 mmol dm^{-3}). The data points correspond to studies where [CN^-] = 0.5 (■), 1.0 (▲), or 2.5 mmol dm^{-3} (●). The data points are connected by guidelines to clarify the trends observed at each concentration of CN^-. These guidelines have no mathematical significance.

reaction is most reasonably attributed to rate-limiting dissociation of the imidazole prior to CN^- binding.

The full rate law for the dissociative mechanism is shown in eq 3, where k_3^{ImH} is the rate constant for dissociation of the imidazole to produce the coordinatively unsaturated FeMo-cofactor intermediate, and k_4 is the rate constant for binding of CN^- to this intermediate. When $k_4[CN^-] > k_{-3}^{ImH}[ImH]$, eq 3 simplifies to eq 4, which has the same mathematical form as that observed experimentally (i.e., $k_3^{ImH} = 50 \pm 10$ s^{-1}).

$$\frac{-\mathrm{d[FeMoco-ImH]}}{\mathrm{d}t} = \frac{k_3^{ImH}k_4[CN^-][\mathrm{FeMoco-ImH}]}{k_{-3}^{ImH}[ImH] + k_4[CN^-]} \quad (3)$$

$$\frac{-\mathrm{d[FeMoco-ImH]}}{\mathrm{d}t} = k_3^{ImH}[\mathrm{FeMoco-ImH}] \quad (4)$$

It is important to note that even when CN^- and FeMoco−ImH are left together for long periods ($\delta = 10$ s, not shown in Figure 6) no further change in k_{obs} for the reaction with PhS^- is observed. Thus, there is no evidence for multiple stages in the reaction of FeMoco−ImH for CN^-.

(b) FeMoco−NMF. The reaction between FeMoco−NMF and CN^- produces FeMoco−CN within the dead time of the apparatus, even when there is only a slight excess of CN^- ([CN^-]/[FeMoco−NMF] = 2.0; [CN^-] = 0.1 mmol dm^{-3}). Consequently, the rate of CN^- reacting with FeMoco−NMF can only be estimated ($k_2^{NMF} \geq 150$ s^{-1}), and the kinetics cannot be determined. The reactivity of FeMoco−NMF is consistent with our proposed dissociative mechanism for the reaction of FeMoco−ImH with CN^- (i.e., that CN^- binds to Mo after dissociation of coordinated NMF). It seems intuitively reasonable that the Mo−NMF bond is more labile than Mo−ImH, resulting in the observed increased reactivity.

(c) FeMoco−CNBu^t. The reaction of FeMoco−CNBu^t with an excess of CN^- shows markedly different kinetics to those described for FeMoco−ImH or FeMoco−NMF. The data illustrating the time course of the reaction between FeMoco−CNBu^t and CN^- are shown in Figure 7. As in Figure 5, the δ axis shows the time PhS^- is added after FeMoco−CNBu^t and CN^- have been mixed. The k_{obs} axis shows the corresponding rate constants for the reaction of PhS^- with the mixture of FeMoco−CNBu^t and CN^- after the time δ.

The data points correspond to rate constants determined under conditions where the entire absorbance−time curves are single exponentials with $k_1^{BuNC} = 50$ s^{-1} or $k_1^{CN} = 2$ s^{-1}. As noted in the earlier section, biphasic traces are observed under all other conditions. Consequently, there are no data points in the intermediate region of Figure 7, only at the extremes. It is evident from Figure 7 that as the concentration of CN^- is increased, the time (δ) necessary to produce FeMoco−CN decreases. Thus, when [CN^-] = 0.5 mmol dm^{-3}, FeMoco−CN is not evident until ca. 250 ms, whereas when [CN^-] = 2.5 mmol dm^{-3}, FeMoco−CN is formed in ca. 50 ms. Inspection of the data in Figure 7 indicates that doubling the concentration of CN^- halves the time necessary to produce FeMoco−CN consistent with the reaction exhibiting a first order dependence on the concentration of CN^-.

The rate law for the reaction of FeMoco−CNBu^t with CN^- is described by eq 5, with $k_2^{BuNC} = (2.5 \pm 0.5) \times 10^4$ dm^3 mol^{-1} s^{-1}. It is important to appreciate that the indirect, sequential-mix method we are using to monitor the reaction between FeMoco−CNBu^t and CN^- means that this dependence on the concentration of CN^- is only approximate. The accuracy of the approach means that while eq 5 certainly describes the principal pathway, an additional minor pathway,

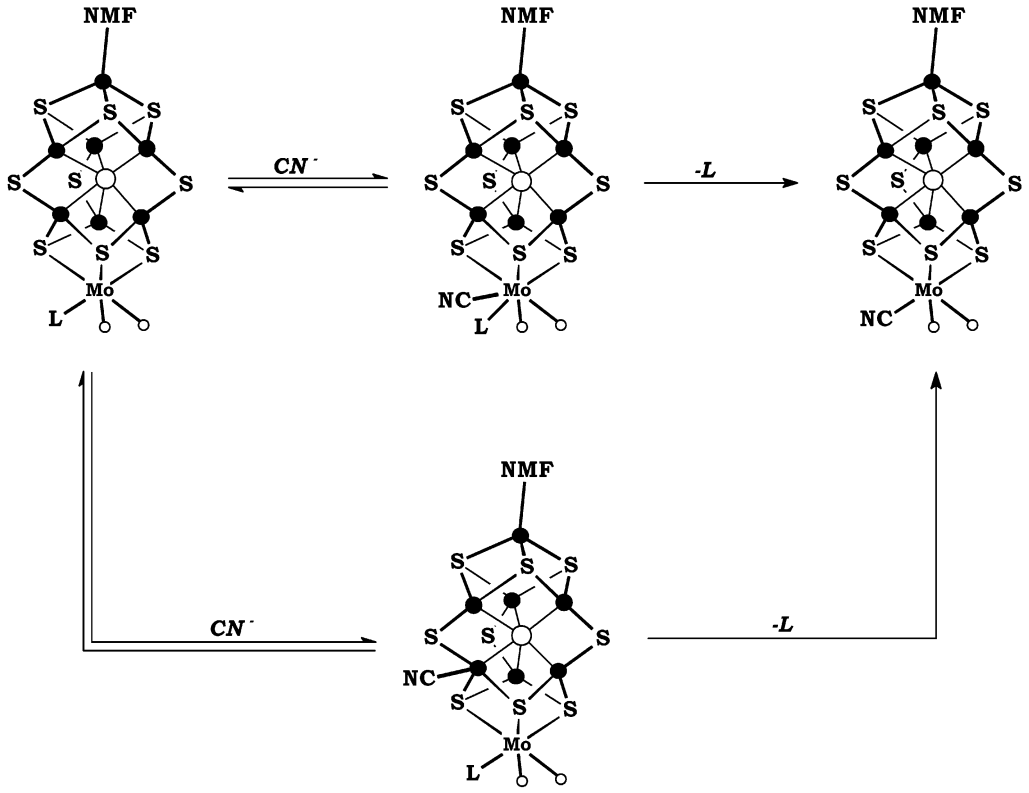

Figure 8. Possible associative pathways for the reaction of CN^- with FeMoco−$CNBu^t$.

independent of the concentration of CN^-, might be undetected.

$$\frac{-\mathrm{d[FeMoco-CNBu^t]}}{\mathrm{d}t} = k_2^{\mathrm{BuNC}}[\mathrm{FeMoco-CNBu^t}][\mathrm{CN^-}] \quad (5)$$

It is worth pointing out, at this stage, that if the kinetics of a substitution reaction exhibit a first order dependence on the concentration of CN^-, this does not rule out a dissociative mechanism.[18] Thus, a mechanism analogous to that shown in Figure 5, in which Bu^tNC initially dissociates from FeMoco−$CNBu^t$ followed by CN^- binding to the vacant site is associated with the rate law shown in eq 6. Equation 6 is obviously analogous to eq 3. If $k_{-3}^{\mathrm{CNBu}}[\mathrm{BuNC}] > k_4[\mathrm{CN^-}]$, eq 6 simplifies to eq 7.

$$\frac{-\mathrm{d[FeMoco-CNBu^t]}}{\mathrm{d}t} = \frac{k_3^{\mathrm{CNBu}}k_4[\mathrm{CN^-}][\mathrm{FeMoco-CNBu^t}]}{k_{-3}^{\mathrm{CNBu}}[\mathrm{Bu^tNC}] + k_4[\mathrm{CN^-}]} \quad (6)$$

$$\frac{-\mathrm{d[FeMoco-CNBu^t]}}{\mathrm{d}t} = \frac{k_3^{\mathrm{CNBu}}k_4[\mathrm{CN^-}][\mathrm{FeMoco-CNBu^t}]}{k_{-3}^{\mathrm{CNBu}}[\mathrm{Bu^tNC}]} \quad (7)$$

Thus, a dissociative mechanism can exhibit a first order dependence on the concentration of CN^- but, under such conditions, must also show an inverse dependence on the concentration of free Bu^tNC. When the reaction between FeMoco−$CNBu^t$ and CN^- is studied in the presence of different concentrations of Bu^tNC ([Bu^tNC] = 1.0−20.0 mmol dm^{-3}), the rate of formation of FeMoco−CN is independent of the concentration of free Bu^tNC. Thus, we can conclude that FeMoco−$CNBu^t$ is not reacting by the dissociative mechanism.

The simplest mechanism consistent with eq 5 is an associative pathway involving attack of CN^- directly at the Mo and displacement of L = Bu^tNC, as shown in the top line of Figure 8. However, eq 5 is also consistent with the more complicated associative mechanism shown on the bottom line of Figure 8. In this more complicated pathway, initial binding of CN^- to the cofactor occurs preferentially to a site other than Mo (a kinetically favored binding site), for example the central Fe sites. With CN^- bound to an Fe, subsequent dissociation of the Mo−$CNBu^t$ bond generates a vacant site on Mo, to which CN^- can now move. On the basis of the kinetic results presented in this paper, it is not possible to establish which of the two pathways shown in Figure 8 operates. We will return to this problem later, when we discuss the results of the theoretical calculations.

The CN^- Binding Sites. It seems most likely that CN^- binds to a metal site on cofactor, and inspection of the structure of FeMo-cofactor indicates three regions of the cluster where CN^- can bind: tetrahedral Fe (by displacing an NMF), one or more of the 6 central Fe's, and Mo. In this section, we consider the kinetic behavior expected for CN^- binding to each of these regions in each of the FeMo-cofactor derivatives.

First, consider the reactivity of the tetrahedral Fe site. For FeMo-cofactor in the MoFe-protein, the Fe at one extreme of the cofactor is coordinated to a cysteinate residue whereas

(18) Espenson, J. H. *Chemical Kinetics and Reaction Mechanisms*; McGraw-Hill: New York, 1981; p 71.

Table 1. Summary of the Rates of Reactions of FeMoco−L (L = NMF, Bu^{t}NC, or Imidazole) with CN^- (k_2^L) and Comparison with the Labilities of Fe−NMF (k_1^L) in the Same Cofactors

FeMoco−L	k_2^L	k_1^L/s^{-1}
FeMoco−NMF	$>150\ s^{-1}$	50 ± 10
FeMoco−CNBu^t	$(2.5 \pm 0.5) \times 10^4$ $dm^3\ mol^{-1}\ s^{-1}$	60 ± 10
FeMoco−ImH	$50 \pm 10\ s^{-1}$	95 ± 10

in extracted FeMo-cofactor a labile (presumably NMF) ligand has replaced this amino acid. Earlier studies show that the rate of the reaction of extracted FeMoco−L with PhS^- at the tetrahedral Fe (k_1^L) depends on the identity of L (where L is bound to Mo). For FeMoco−NMF, FeMoco−CNBu^t, and FeMoco−ImH, the values of k_1^L are shown in Table 1,[13] and compared with the rates of reactions with CN^- (k_2^L). It is evident that there is no correlation between the values of k_1^L and k_2^L. With FeMoco−NMF, the reaction with CN^- is at least 3 times faster than the rate of Fe−NMF dissociation, whereas in FeMoco−ImH the reaction with CN^- is 2 times slower than the dissociation of the Fe−NMF bond in this derivative. Thus, although FeMoco−ImH rapidly generates a vacant site at the tetrahedral Fe ($k_1^{ImH} = 92\ s^{-1}$), binding of CN^- waits for the slower dissociation of the Mo−ImH bond ($k_2^{ImH} = 50\ s^{-1}$) before it binds to the cofactor. The rate at which CN^- binds to FeMoco−L is independent of how rapidly a vacant site is generated at the tetrahedral Fe. The conclusion must be that CN^- is not binding to the tetrahedral Fe site of FeMoco−L.

Several theoretical calculations[6] and experimental studies on altered nitrogenase MoFe-proteins have emphasized the potential of the central Fe atoms as possible substrate binding sites. Consideration of the structure of FeMoco−L shows that, when bound to Mo, L is too remote from the central Fe's to interfere sterically with CN^- binding to Fe at either the Fe_4S_3 or the $MoFe_3S_3$ end of the cofactor. Specifically for FeMoco−ImH, if the kinetically favored binding site for CN^- were any of the central Fe atoms, it is difficult to see why dissociation of imidazole is an essential prerequisite to substrate binding. It is much more reasonable that imidazole must dissociate from FeMoco−ImH prior to CN^- binding because imidazole is occupying the site (Mo) where CN^- wants to bind, and that the imidazole is sufficiently labile that it will dissociate.

While the kinetics of the reaction between CN^- and FeMoco−ImH indicate Mo is the kinetically favored binding site for CN^-, for the other derivatives the initial binding site is more ambiguous. It seems reasonable for FeMoco−NMF that the Mo−NMF bond is sufficiently labile that dissociation of this bond precedes the direct binding of CN^- to Mo. However, for FeMoco−CNBu^t the kinetics indicate an associative mechanism, but whether initial CN^- attack is at Mo or an Fe atom cannot be decided from the kinetics alone. Model structures, based on the geometries obtained from DFT calculations, reveal marked steric congestion around Mo in FeMoco−CNBu^t (Figure 9) and mitigate against direct attack of CN^- at Mo.

Mo−L Bond Strengths: DFT Calculations. We have obtained a theoretical description of the energetics of cyanide

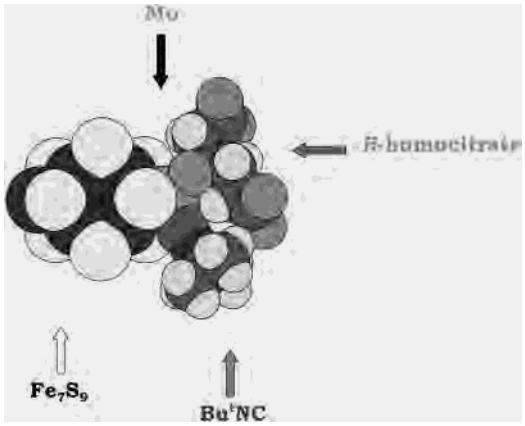

Figure 9. Space-filling structure of FeMoco−CNBu^t showing the steric congestion around the Mo site. The Mo end of the cofactor with the *R*-homocitrate and Bu^{t}NC ligand is shown on the right-hand side of the figure.

binding to the different metal sites of extracted FeMo-cofactor by means of DFT calculations on fragments of the FeMoco. Larger models would of course be better, but the time required for the calculations scales approximately as the third or fourth power of the number of basis functions. Furthermore, as the number of metals is increased the number of possible spin state permutations increases rapidly. Hence, a full treatment of cyanide binding to the cofactor would be extremely expensive. Comparison of published calculations on whole FeMoco with smaller models indicates that the latter are of sufficient accuracy to be of qualitative value.

For the central Fe and Mo sites, a $[(HS)Fe(SH)_2Mo(SH)(OCH_2CO_2)]$ model was used, while the tetrahedral Fe site was modeled using a $[Fe(SH)_3]$ fragment.[20] The calculation of absolute values for the cyanide binding energies is complicated by the charge on the CN^- ion. An important consideration in our choice of the calculation model systems is that, for the cluster fragments, there are fewer geometric restraints because some of the bonds are absent. This allows large distortions when the overall energy is relatively insensitive to, for example, a particular bond angle. The distortions always tend to be much worse for charged species than neutral, because of electrostatic repulsions. This is quite a routine problem and can be addressed either by including extra geometrical restraints, or by keeping the fragment neutral. We prefer the second option as it allows for distortions, which might occur for other, more mechanistically relevant, reasons. More important, the calculation of absolute binding energies for charged species would require explicit consideration of solvation energies. Hence for the purposes of the present study, we have confined our efforts to the calculation of relative binding energies for the different metal sites. These can be readily obtained by calculation of the bond dissociation energies for the $CN^\bullet$ radical rather than

(19) (a) Dance, I. *Chem. Commun*. **2003**, 324. (b) Hinnemann, B.; Nørskov, J. K. *J. Am. Chem. Soc.* **2003**, *125*, 1466 and references therein.

(20) Truncation with H atoms is routinely used for calculations of this type in order to model the inner coordination spheres of the metal centers at reasonable cost. This approach appears to be valid for FeMo-cofactor in that the calculated properties of the metal sites (e.g., with respect to N_2 binding) are not seen to vary greatly with the level of truncation of the model (cf. ref 6).

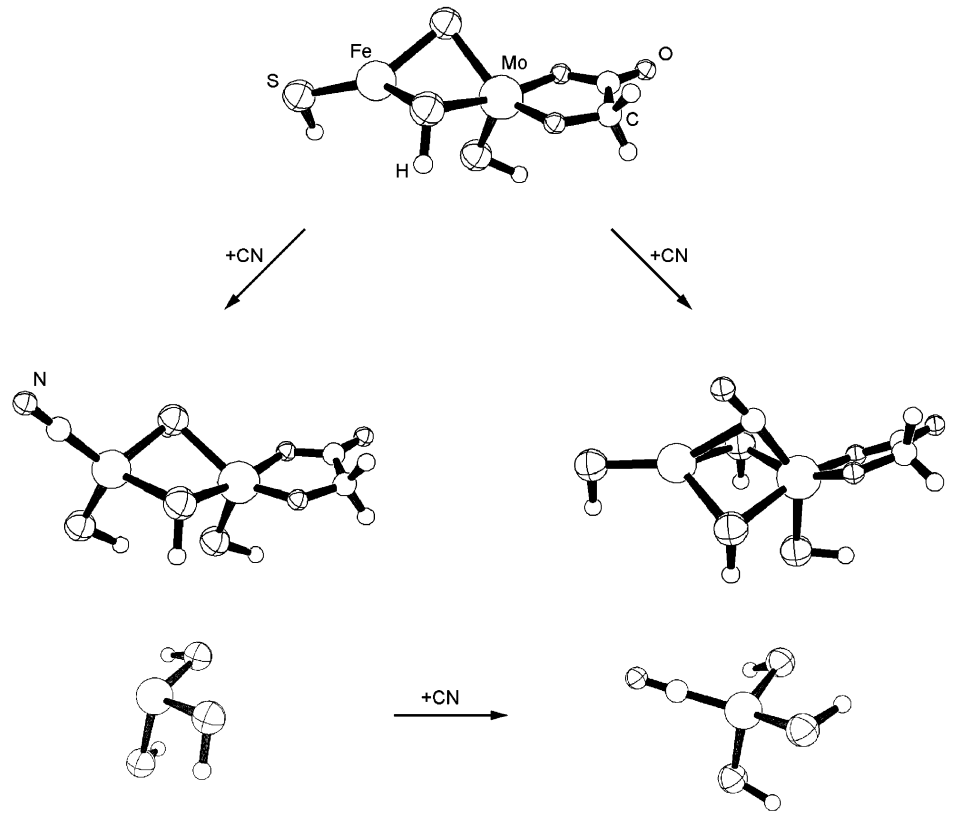

Figure 10. Structures calculated using density functional theoretical calculations on fragments of FeMo-cofactor, for the binding of CN^- to the three different types of metal sites (tetrahedral Fe, central Fe's, and Mo). The figure was constructed using ORTEP-3 for Windows [Farrugia, L. J. *J. Appl. Crystallogr.* **1997**, *30*, 565].

Table 2. Calculated M−CN Bond Dissociation Energies for Cyanide Ligands at Various Sites of FeMoco

CN binding site	M−CN bond dissociation energy/kcal mol^{-1}
Mo no constraints	68
Mo Fe atom fixed as planar	69
Mo S−Mo−S angles fixed	59
central Fe no constraints	56
central Fe Fe atom fixed as planar	46
central Fe S−Mo−S angles fixed	56
tetrahedral Fe	54

the CN^- ion, so avoiding the charge-associated problems already mentioned. For each structure, several spin state combinations were considered (up to four states). For the FeMo fragment, the different spin states generally gave similar energies; antiferromagnetic coupling of the Mo and Fe spins was marginally preferred over ferromagnetic coupling (by 1−2 kcal mol^{-1}). The ground state structures are shown in Figure 10, and the M−CN bond dissociation energies (BDEs) are compared in Table 2.

Although we have not attempted to include the effects of the newly discovered central C, N, or O atom of the FeMoco in the present calculations, it is worth considering how this might perturb the results. Obviously, including the central light atom would change the results of the calculations; however, it would tend to strengthen the case for Mo rather than weaken it, since the central Fe atoms can no longer be considered as three-coordinate and therefore potentially unusually reactive. Very recent theoretical studies[19] indicate that the central atom is most likely to be N, in line with the experimental assignment.[5] The observation that the six central Fe atoms of the FeMoco are formally four- rather than three-coordinate suggests that the three-coordinate model we have used would, if anything, overestimate their ability to bind species such as cyanide. This certainly seems to be the case for neutral species, where changing the inner coordination sphere of Fe atoms from FeS_3 to FeS_3N results in smaller calculated binding energies[22] for both CO and C_2H_2. DFT calculations on binding of acetylene and CO to the central Fe sites indicate that the binding energies are lower when the central atom (assumed to be N) is included.[22] In the case of CO, which is isoelectronic with cyanide, the binding energy is reduced by approximately 7 kcal/mol.

As shown in Figure 10, coordination of cyanide induces distortions in the structure. Most noticeably, the central Fe site becomes tetrahedral, while for cyanide on Mo, the SH group *trans* to the cyanide ligand moves such that the angles between the terminal and bridging Mo−S bonds become more acute (83.1° compared to a mean value of 102.3° from the *K. pneumoniae* X-ray crystal structure).[12] The model is intrinsically more flexible than the whole FeMoco, and this is probably reflected in these relatively large distortions. In order to estimate the effects of this extra flexibility on the results, further calculations were carried out on the ground

(21) (a) Christensen, J.; Cash, V. L.; Seefeldt, L. C.; Dean, D. R. *J. Biol. Chem.* **2000**, *275*, 11459. (b) Christensen, J.; Seefeldt, L. C.; Dean, D. R. *J. Biol. Chem.* **2000**, *275*, 36104. (c) Mayer, S. M.; Niehaus, W. G.; Dean, D. R. *J. Chem. Soc., Dalton Trans.* **2002**, 802.

(22) Durrant, M. C. Unpublished work.

spin states, using additional geometry constraints; in one set of calculations, the central Fe atom was constrained to be planar, and in the second, the angles between the terminal and bridging Mo−S bonds was fixed at 102.3°. The results shown in Table 2 show that in all cases cyanide has a clear preference for the Mo site. The Mo site exhibits a strong *trans* interaction between the CN and terminal SH ligands; however, even in the most unfavorable case where the S−Mo−S angles are completely rigid, cyanide still prefers Mo. The Fe−CN BDEs for the central and tetrahedral Fe sites are comparable, provided that the central Fe site is allowed to assume a tetrahedral geometry; when this site is constrained to be planar, the BDE falls off markedly. DFT calculations[19] on the binding of N_2 and CO to a more complete model of the FeMoco showed similar distortions of the central Fe sites toward tetrahedral. Hence, the results of the DFT calculations agree with the interpretation of the kinetic data that cyanide prefers to bind at molybdenum.

A noteworthy feature of the Mo cyanide structure in Figure 10 is that the cyanide has adopted a semibridging geometry. When exploring the geometry of the bound cyanide, this semibridging configuration is observed as a minimum despite the fact that the optimization was started with a purely terminally bound cyanide. The calculated Mo−C and Fe−C distances of 2.10 and 2.45 Å, respectively, show that the interaction with the trigonal Fe is in this case relatively weak. A similar bridging geometry was calculated for the diazenido(1−) ligand when bound at Mo (i.e., MoNNH).[6b] In the diazenido case, however, the bridging interaction was η^2, involving the lone pair of the β-nitrogen, and hence more pronounced.

The DFT calculations were extended, using the same methodology, to compare the M−L BDEs for [(HS)Fe-$(SH)_2$Mo(L)(SH)(OCH_2CO_2)] fragments, where L = CNMe or imidazole. Given the relatively small energy difference between the antiferromagnetic and ferromagnetic states for the binuclear species shown in Figure 10, these calculations were limited to the antiferromagnetically coupled states only.[23] The calculated Mo−L BDEs for the species where L = CNMe or imidazole were 27 and 37.5 kcal mol^{-1}, respectively. Hence, dissociation of imidazole from the Mo site of FeMo-cofactor is predicted to be significantly harder than the dissociation of isonitrile. It should be noted that these calculations do not allow a direct comparison of the affinities of the Mo site for imidazole and alkyl isonitrile with that for cyanide, since free cyanide is anionic and will therefore have very different solvation properties.

Factors Controlling CN^- Binding Site on FeMoco−L. Herein we have reported the first kinetic study on the binding of a nitrogenase substrate to extracted FeMo-cofactor in NMF. The results from the kinetic and DFT studies are consistent with the unified picture for the reactions of CN^- with all FeMoco−L presented in Figure 11. In this figure, binding of CN^- can occur either directly to the six-coordinate Mo in FeMoco−L by a dissociative mechanism involving initial dissociation of L, or by an associative mechanism where CN^- binds initially to one or more of the central Fe sites and subsequent dissociation of L allows CN^- to move to Mo. Clearly, the factors controlling which site CN^- binds to are (i) the lability of the Mo−L bond and (ii) the electronic effect of L on the cluster core. The relative bond strengths of Mo−imidazole and Mo−isonitrile have already been discussed. Taking the theoretical and experimental evidence together, we conclude that the relatively strong FeMoco−imidazole interaction results in weaker binding of CN^- at the Fe sites. Hence, CN^- binding has to await Mo−ImH dissociation via the upper pathway. In contrast, the weaker electron-releasing effect of coordinated isonitrile allows CN^- to bind to the Fe site(s) of FeMoco−$CNBu^t$. Consequently, the reaction of CN^- with FeMoco−$CNBu^t$ occurs principally by the bottom pathway. Finally, with FeMoco−NMF, it seems likely that the Mo−NMF bond breaks sufficiently rapidly that the reaction with CN^- goes exclusively by the top pathway.

Studies on FeMoco−L and the Action of Nitrogenase. The discussion presented here for the reaction of CN^- with a variety of different extracted FeMo-cofactor derivatives indicates that CN^- can bind to at least two sites on the cluster in the semireduced redox level: the Mo and presumably one of the Fe atoms in the center of the cofactor. DFT calculations indicate that both steric and electronic factors influence where initially CN^- binds. There are previous kinetic studies on any substrate binding to extracted FeMo-cofactor with which to compare our results. In this section, we will explore how our results on extracted FeMo-cofactor relate to the action of the cofactor in the MoFe-protein. There are two related, but distinct, aspects that need to be addressed: (i) What does work on extracted FeMo-cofactor tell us in general terms about the binding of substrates to the active site? (ii) How do the results presented herein specifically relate to the binding of CN^- by the enzyme?

The Mo-nitrogenase Glyα69 and Alaα70 residues are contained in the active site cavity, close to the FeMo-cofactor and sitting over the central Fe_4S_4 faces. Recent studies on altered nitrogenase MoFe-proteins (where the Glyα69 and Alaα70 are substituted) have led to the proposal that alkynes bind to FeMo-cofactor on one of the central Fe_4S_4 faces.[21] Clearly, this is in contrast to our results presented herein which indicate that no Fe atom is the *final* binding site for CN^-. While it is possible that different substrates bind at physically different sites on the cofactor, there could be other reasons for a difference between studies on the enzyme and the extracts which need to be considered.

Extracted FeMo-cofactor undoubtedly contains more labile ligands than the cofactor bound to the MoFe-protein. The two cofactor-ligating amino acids Cysα273 and Hisα440 in the protein have been replaced (presumably by NMF) in extracted FeMo-cofactor. The lability of these nonprotein ligands on extracted FeMo-cofactor could produce a reactivity not possible in the enzyme. In addition, our studies on extracted FeMo-cofactor are restricted to the semireduced state ($S = {}^3/_2$ spin state). In contrast, studies on the enzyme show that as it turns over it allows the substrate access to

(23) Lee, H.-I.; Hales, B. J.; Hoffman, B. M. *J. Am. Chem. Soc.* **1997**, *119*, 11395.

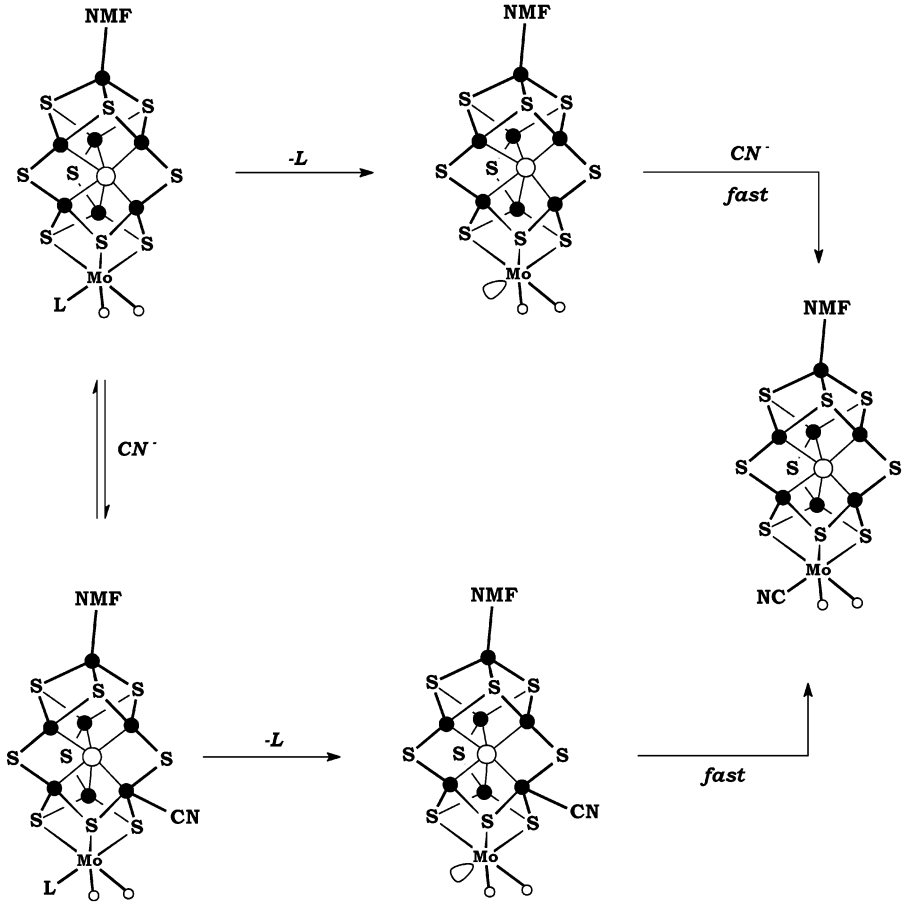

Figure 11. Unified picture for reactions between CN^- and FeMoco−L (L = NMF, Bu^{t}NC, or imidazole).

the cofactor in a variety of different redox states. It is possible that a change in the redox state of FeMo-cofactor affects the relative affinities of different regions of the cluster toward substrates.

In addition to the problems of redox state and ancillary ligands in using extracted FeMo-cofactor as a model for the active site in nitrogenase, there are other limitations. Most notably, the reactions of extracted FeMo-cofactor are studied in NMF as the solvent. There is little data about the acid−base properties of species in NMF. Consequently, in the studies with CN^- we have not varied the pH of the solution and hence cannot establish whether the substrate is HCN or CN^-. This is an important consideration since earlier studies indicated that HCN is a substrate for nitrogenase while CN^- is an inhibitor.[24]

The pre-steady-state kinetics of HCN reduction by *Azotobacter vinelandii* nitrogenase, and CN^- inhibition of the total electron flow through nitrogenase, have been investigated.[24] The characteristic features of the enzyme's behavior in the presence of CN^- are a 100 ms lag before H_2 is detected (as is observed in the absence of CN^-), and a further 3 s lag before electron flow is inhibited by CN^- or the reduction product (CH_4) is observed.

The generally accepted mechanism for nitrogenase[24,25] indicates that lag times are affected by both the redox state of the MoFe-protein and the number of electrons transferred. Using the previously established rate constants for the elementary reactions involved in turnover, the lag times can be calculated. Applying these criteria to the results for the reduction of cyanide by nitrogenase shows that the delays are equivalent to ca. 20 electron transfer steps. This is clearly unreasonable in terms of a catalytic cycle, and it has been suggested that some additional slow processes must occur before reduction of cyanide, or inhibition of electron flow, can occur. It has been proposed that the slow steps involve cyanide binding by replacing one or more ligands on the cofactor. Clearly, this would be a ligand that is not displaced by dinitrogen since studies on nitrogenase reduction of dinitrogen shows ammonia is produced much more rapidly.

The studies described in this paper show that CN^- binding to extracted FeMoco−ImH has to await the dissociation of imidazole. For the FeMo-cofactor inside the *K. pneumoniae* protein, Mo is coordinated by the imidazole residue of Hisα440. We have investigated the plausibility of cyanide binding to the Mo site via displacement of this residue, using INSIGHT-II molecular modeling software[26] and the Mo−CN geometry derived from the DFT calculations. We find that on breaking the Mo−ImH bond by rotations about the Hisα440 side chain CH_2−C bonds, cyanide can indeed be

(24) Lowe, D. J.; Fisher, K.; Thorneley, R. N. F.; Vaughn, S. A.; Burgess, B. K. *Biochemistry* **1989**, *28*, 8460.

(25) Thorneley, R. N. F.; Lowe, D. J. *Molybdenum Enzymes*; Spiro, T., Ed.; Wiley-Interscience: New York, 1985; p 221.

(26) *INSIGHT II*; Accelrys Ltd.: Cambridge, U.K., 2001.

accommodated at Mo, adopting a semibridging interaction with an Fe atom, and no significant steric clashes within the protein. Whether CN^- binding to Mo represents the prequel to CN^- transformation or the inhibition pathway is not clear. It seems intuitively reasonable that cleavage of the Mo−Hisα440 bond could be sufficiently slow to lead to the long lag times observed with the enzyme.

Finally, it is worth commenting on our observation that electronic factors (i.e., electron-richness of the cluster) affect where CN^- initially binds to the extracted FeMo-cofactor derivatives. There is evidence that the cofactor in the MoFe-protein is sensitive to subtle changes in its environment which could affect the electron-richness of the active site.

Studies on an altered MoFe-protein (Glnα195 replacing Hisα195) show that although reduction of cyanide is not impaired by this substitution, cyanide inhibition of the total electron flow to substrate is completely absent.[27] The residue Hisα195 is close to FeMo-cofactor and is only hydrogen-bonded to one of the sulfur atoms of the cluster. Hisα195 is a hydrogen-bond donor residue. Replacement of Hisα195 by another amino acid (Glnα195) is likely to affect the electron-richness of the cofactor and hence influence its interactions with substrates. In extreme cases, it seems plausible that this electronic effect could stop the substrate binding or change the position of the binding site on the cofactor. Certainly, previous studies on synthetic Fe−S-based clusters[28] and extracted FeMo-cofactor[29] have shown that protonation of the clusters affects their reactivity. In addition, hydrogen-bonding to extracted FeMo-cofactor has been shown to influence the reactivity of the cofactor.[13b]

Acknowledgment. We thank the John Innes Foundation for a studentship (Z.C.) and the University of Newcastle for a studentship (A.J.D.). B.E.S. thanks the John Innes Foundation and the Leverhulme Trust for Emeritus Fellowships.

Supporting Information Available: Computational and kinetic data. This material is available free of charge via the Internet at http://pubs.acs.org.

IC030108Q

(27) Dilworth, M. J.; Fisher, K.; Kim, C.-H.; Newton, W. E. *Biochemistry* **1998**, *37*, 17495.

(28) (a) Henderson, R. A.; Oglieve, K. E. *J. Chem. Soc., Chem. Commun.* **1994**, 377. (b) Grönberg, K. L. C.; Henderson, R. A. *J. Chem. Soc., Dalton Trans.* **1996**, 3667. (c) Henderson, R. A.; Oglieve, K. E. *J. Chem. Soc., Dalton Trans.* **1998**, 1731.

(29) Almeida, V. R.; Gormal, C. A.; Grönberg, K. L. C.; Henderson, R. A.; Oglieve, K. E.; Smith, B. E. *Inorg. Chim. Acta* **1999**, *291*, 212.